The Protein Kinase Cβ–Selective Inhibitor, Enzastaurin (LY317615.HCl), Suppresses Signaling through the AKT Pathway, Induces Apoptosis, and Suppresses Growth of Human Colon Cancer and Glioblastoma Xenografts

Jeremy R. Graff, Ann M. McNulty, Kimberly Ross Hanna, Bruce W. Konicek, Rebecca L. Lynch, Spring N. Bailey, Crystal Banks, Andrew Capen, Robin Goode, Jason E. Lewis, Lillian Sams, Karen L. Huss, Robert M. Campbell, Philip W. Iversen, Blake Lee Neubauer, Thomas J. Brown, Luna Musib, Sandaruwan Geeganage, and Donald Thornton

Lilly Research Labs, Eli Lilly and Company, Indianapolis, Indiana

Abstract

Activation of protein kinase Cβ (PKCβ) has been repeatedly implicated in tumor-induced angiogenesis. The PKCβ-selective inhibitor, Enzastaurin (LY317615.HCl), suppresses angiogenesis and was advanced for clinical development based upon this antiangiogenic activity. Activation of PKCβ has now also been implicated in tumor cell proliferation, apoptosis, and tumor invasiveness. Herein, we show that Enzastaurin has a direct effect on human tumor cells, inducing apoptosis and suppressing the proliferation of cultured tumor cells. Enzastaurin treatment also suppresses the phosphorylation of GSK3β^{ser9}, ribosomal protein S6$^{S240/244}$, and AKT^{Thr308}. Oral dosing with Enzastaurin to yield plasma concentrations similar to those achieved in clinical trials significantly suppresses the growth of human glioblastoma and colon carcinoma xenografts. As in cultured tumor cells, Enzastaurin treatment suppresses the phosphorylation of GSK3β in these xenograft tumor tissues. Enzastaurin treatment also suppresses GSK3β phosphorylation to a similar extent in peripheral blood mononuclear cells (PBMCs) from these treated mice. These data show that Enzastaurin has a direct antitumor effect and that Enzastaurin treatment suppresses GSK3β phosphorylation in both tumor tissue and in PBMCs, suggesting that GSK3β phosphorylation may serve as a reliable pharmacodynamic marker for Enzastaurin activity. With previously published reports, these data support the notion that Enzastaurin suppresses tumor growth through multiple mechanisms: direct suppression of tumor cell proliferation and the induction of tumor cell death coupled to the indirect effect of suppressing tumor-induced angiogenesis. (Cancer Res 2005; 65(16): 7462-9)

Introduction

The protein kinase C (PKC) family of serine-threonine protein kinases has been repeatedly implicated in the processes that control tumor cell growth, survival, and progression (reviewed in ref. 1). Early observations that PKCs are activated by tumor-promoting phorbol esters suggested that PKC activation may be involved in tumor initiation and progression (2). Tumor-induced angiogenesis requires activation of PKCs, particularly PKCβ (1). Vascular endothelial growth factor (VEGF)–induced hepatocellular carcinoma growth can be suppressed by treatment with the PKCβ-selective inhibitor LY333531, which elicits cell death in these hepatocellular carcinoma tissues (3).

PKC activation also contributes to tumor cell survival and proliferation and has been repeatedly implicated in the malignant progression of human cancers, notably B cell lymphomas (4), malignant gliomas (5), and colorectal carcinomas (6). PKCβ expression is specifically increased in patients with fatal/refractory diffuse large B cell lymphoma (DLBCL), linking increased PKCβ expression to decreased patient survival (4). Further supporting a role for PKCβ in DLBCL, cultured DLBCL cells with PKCβ overexpression undergo apoptosis when treated with the PKCβ-selective inhibitor LY379196 (7). In intestinal epithelia, expression of a PKCβ transgene elicits hyperproliferation of the colonic epithelium and increases susceptibility to carcinogen-induced colon carcinogenesis indicating that PKCβII can promote colon carcinogenesis (6, 8). Furthermore, PKCβII expression in rat intestinal epithelial cells can induce an invasive phenotype (9).

Although PKC activation has been implicated in tumor formation and progression, the signaling pathways affected by PKC activation that contribute to malignancy are unclear. PKC activation can trigger signaling through the ras/extracellular signal-regulated kinase (ERK) pathway, which may be involved in the controlling cellular proliferation and apoptosis (1) as well as the induction of intestinal cell invasiveness (9). PKCβII activity may also play a role in reducing the sensitivity of intestinal epithelia to the growth suppressive effects of transforming growth factor β (8). Recent work has now shown a link between PKC activity and activity of the phosphatidylinositol 3-kinase (PI3K)/AKT pathway, a prominent regulatory pathway governing the apoptotic response. PKC activation requires phosphorylation of the T-loop, a process triggered by the activity of phosphatidylinositol-dependent kinase-1 (PDK-1), a key effector kinase-activated immediately downstream of PI3K (10). PKCα, PKCβ, and PKCη can also directly phosphorylate AKT at Ser^{473}, which is essential for AKT activity (11–13). Moreover, both PKC (14, 15) and AKT (16) can phosphorylate glycogen synthase kinase 3β at Ser^{9} (GSK3β), further supporting the notion that these signaling pathways overlap. Crosstalk between PKC and the PI3K/AKT pathway may be an attractive mechanism by which PKCs influence the apoptotic response.

Requests for reprints: Jeremy R. Graff, Principal Research Scientist, Cancer Growth and Translational Genetics, Oncology Division, Lilly Research Labs, Lilly Corporate Center, DC0546, Indianapolis, IN 46285. Phone: 317-277-0220; Fax: 317-277-3652; E-mail: graff_jeremy@lilly.com.

doi:10.1158/0008-5472.CAN-05-0071

Collectively, these data have implicated PKCs in tumor progression and have prompted the development of novel anticancer therapeutics targeting PKC. Enzastaurin (LY317615.HCl) was developed as a selective PKCβ inhibitor (17). Based upon the role established for PKCβ in angiogenic signaling (1, 3), enzastaurin was initially evaluated in preclinical tumor models for antiangiogenic activity. Enzastaurin treatment dramatically suppressed the growth of new vasculature towards a VEGF-impregnated disc implanted in the rat corneal micropocket (18). Enzastaurin also decreased microvessel density and VEGF expression in human tumor xenografts (19). The striking antiangiogenic effects of enzastaurin prompted the clinical development of enzastaurin.

In addition to the antiangiogenic effects of enzastaurin, we now show that enzastaurin directly suppresses proliferation and induces apoptosis of tumor cells in culture and suppresses phosphorylation of GSK3β, ribosomal protein S6, and AKT. Oral dosing of enzastaurin to achieve plasma concentrations of drug comparable with those achieved in clinical trials significantly suppresses the growth of human colon and glioblastoma xenografts. As in cell culture, GSK3β phosphorylation was suppressed in these tumor tissues. Moreover, GSK3β phosphorylation was suppressed to a similar extent and with a similar time course in peripheral blood mononuclear cells (PBMCs) from these xenograft-bearing mice. These data support the notion that enzastaurin elicits an antitumor effect by suppressing signaling through the AKT pathway, directly inducing tumor cell death and suppressing tumor cell proliferation.

Materials and Methods

Kinase inhibition assays. The inhibition of PKCβII, PKCα, PKCε, or PKCγ activity by enzastaurin was determined using a filter plate assay format measuring ^{33}P incorporation into myelin basic protein substrate. Reactions were done in 100-μL reaction volumes in 96-well polystyrene plates with final conditions as follows: 90 mmol/L HEPES (pH 7.5), 0.001% Triton X-100, 4% DMSO, 5 mmol/L $MgCl_2$, 100 μmol/L $CaCl_2$, 0.1 mg/mL phosphatidylserine (Avanti Polar Lipids, Alabaster, AL), 5 μg/mL diacetyl glyerol (Avanti Polar Lipids), 30 μmol/L ATP, 0.005 μCi/μL ^{33}ATP (NEN, Boston, MA), 0.25 mg/mL myelin basic protein (Sigma, St. Louis, MO), serial dilutions of enzastaurin (1-2,000 nmol/L), and recombinant human PKCβII, PKCα, PKCε, or PKCγ enzymes (390, 169, 719, or 128 pmol/L, respectively; PanVera, Madison, WI). Reactions were started with enzyme addition, incubated at room temperature for 60 minutes, quenched with 10% H_3PO_4, transferred to multiscreen anionic phosphocellulose 96-well filter plates (Millipore, Billerica, MA), incubated 30 to 90 minutes, filtered, and washed with 4 volumes of 0.5% H_3PO_4 on a vacuum manifold (Millipore). Scintillation cocktail was added and plates were read on a Microbeta scintillation counter (Wallac, Turku, Finland). IC_{50} values were determined by fitting a three-variable logistic equation to the 10-point dose-response data using ActivityBase 4.0 (ID Business Solutions, Ltd., Cambridge, MA).

Upstate Kinase Profiler data were derived as per the provider (Upstate, Charlottesville, VA). Data are presented as the percent of kinase activity without enzastaurin.

Cell culture. HCT116 human colorectal cancer, U87MG human glioblastoma, and PC3 human prostatic adenocarcinoma cells were obtained from the American Type Culture Collection (ATCC, Manassas, VA) and cultured in media with fetal bovine serum (FBS; Hyclone, Logan, UT) without antibiotics, as prescribed (ATCC).

Xenograft tumor studies. Five million HCT116 human colon cancer cells or U87MG human glioblastoma cells were injected s.c. in the flank of female, 6 to 8 weeks old, athymic nude mice (Harlan, Indianapolis, IN) in a 1:1 mixture of serum-free growth media and matrigel (Becton Dickinson, Bedford, MA). Mice were monitored daily for palpable tumors. Enzastaurin treatment was initiated when the tumors reached a group mean of 100 mm^3. Enzastaurin was suspended in 10% acacia (Fisher Scientific, Fair Lawn, NJ) in water and dosed by gavage twice daily at 75 mg/kg based upon weekly body measurements for each treated group. Control groups were treated only with vehicle.

Protein lysates from cells and *in vivo* tissues. Lysates for western blot experiments and ELISA assays were prepared using Biosource Cell Extraction Buffer (Biosource International, Camarillo, CA) plus protease inhibitor cocktails (Sigma P8340, P2850, P5726) at 10 μL of each per mL of cell extraction buffer (complete lysis buffer). Extracted tumors from *in vivo* studies were placed in 1 mL of ice-cold complete lysis buffer in Bio-101 tubes (QBiogene, Irvine, CA) for immediate homogenization. The Fast Prep FP-120 instrument (QBiogene) homogenized the tissues during two 30-second blasts. The homogenate was then transferred to Eppendorf tubes and centrifuged 10 minutes at 12,000 rpm. The supernatant (protein lysate) was then saved for western blotting or ELISA. The Bio-Rad DC-Protein assay kit (Bio-Rad, Hercules, CA) was used to determine protein concentrations.

PBMCs from the HCT116 tumor-bearing mice treated with enzastaurin were isolated as per the manufacturer's protocol included with the BD Vacutainer CPT tubes (BD, Franklin Lakes, NJ). Briefly, blood from five identically treated mice was pooled into a single CPT tube and centrifuged at 1,800 RCF for 30 minutes to separate blood components. The PBMC layer was collected and washed with 5 mL of ice-cold D-PBS, centrifuged 10 minutes at 200 rpm, and resuspended in 250 μL of complete lysis buffer. After centrifugation, the supernatant was collected for protein analysis.

Western blot and ELISA assays. The following antibodies used for western blotting were phosphoGSK3β^{Ser9}, S6 ribosomal protein, phosphoS6$^{Ser240/244}$, and phosphoAKT^{Thr308} (Cell Signaling Technologies, Beverly, MA). Antibodies for total GSK3β and total AKT were purchased from BD Biosciences (San Jose, CA). Western blots were done as described (20).

Proliferation assays. Proliferation was assessed for all cell lines over a 6-day time course in media supplemented with 1% FBS (7 days total). Briefly, 1,000 cells were plated per well in a 96-well plate and changed to fresh media (1% FBS) with or without enzastaurin on days 1 and 4. On day 7, the media were removed and 100 μL propidium iodide (PI) solution (10 μg/mL in D-PBS) were added to each well. An initial reading for PI staining (excitation at 500 nmol/L, absorbance at 615 nmol/L) was done using the WallacVictor plate reader following a 30-minute incubation to determine the nonviable cell fraction. The plate was then frozen at −80 °C for 2 hours, thawed, and reread. The proliferative index was scored by subtracting the prefreeze data (nonviable cells) from the postfreeze data (all cells).

Apoptosis assays. Apoptosis induction by enzastaurin was measured by nucleosomal fragmentation (Cell Death Detection ELISA^{plus}, Roche Applied Science, Indianapolis, IN) and terminal deoxynucleotidyl transferase–mediated nick-end labeling (TUNEL) staining for HCT116 and U87MG cell lines. Briefly, 5,000 cells were plated per well in 96-well plates (1% FBS-supplemented media conditions), incubated with or without enzastaurin for 48 to 72 hours (as indicated) and run as per the manufacturer's protocol (Roche Applied Science). The absorbance values were normalized to those from control-treated cells to derive a nucleosomal enrichment factor at all concentrations as per the manufacturer's protocol (Roche Applied Science). The concentrations studied ranged from 0.1 to 10 μmol/L. *In situ* TUNEL staining was assayed with the *In situ* Cell Death Detection, Fluorescein kit (Roche Applied Science). Cells (75,000) were plated per well in 6-well plates and incubated 72 hours in 1% FBS-supplemented media ± enzastaurin. Fluorescein-labeled DNA strand breaks were detected with the BD epics flow cytometer. Ten thousand, single-cell, FITC-staining events were collected for each test.

PhosphoGSK3β^{Ser9} ELISA. Lysates prepared from HCT116 and U87MG tumors or mouse PBMCs were prepared as described above. PhosphoGSK3β^{Ser9} was quantitated using the Assay Design, Inc. (Ann Arbor, MI) immunometric assay kit. Briefly, 15 μL of tumor lysate (400-600 μg protein per well) or 25 μL PBMC lysate (50-100 μg protein per well) were added to all test wells. Absolute phosphoGSK3β^{Ser9} values are reported in pg phosphoGSK3β^{Ser9}/mg lysate.

Statistical analyses. Tumor volume data are transformed to a log scale to equalize variance across time and treatment groups. The log volume data are analyzed with a two-way repeated-measures ANOVA by time and treatment using SAS PROC MIXED software (SAS Institute, Inc., Cary, NC). Treatment groups are compared with the control group at each time point. The data are

Table 1. Enzasturin (LY317615.HCl) structure and PKC inhibition (IC_{50}, μmol/L)

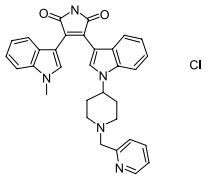

PKCβ	PKCα	PKCγ	PKCε
0.006	0.039	0.083	0.110

NOTE: IC_{50} values were calculated from a 10-point curve from filter-binding assays run at 30 μmol/L ATP.

plotted as means and SEs for each treatment group versus time. Statistical significance for the effect of enzastaurin treatment on GSK3β phosphorylation in xenograft tumors was assessed by Dunnett's method, one-way ANOVA (JMP Statistical Discovery Software, SAS Institute).

Results

Enzastaurin treatment suppresses tumor cell proliferation and induces apoptosis. PKCβ activity has been implicated in tumor-induced angiogenesis (1, 3). Enzastaurin was developed as an ATP-competitive, selective inhibitor of PKCβ with an IC_{50} for PKCβ of 6 nmol/L (Table 1). As such, enzastaurin was developed as an antiangiogenic therapy for cancer (17–19). PKC activation has now been implicated in tumor cell proliferation and apoptosis as well (1). We therefore sought to examine whether enzastaurin would also show direct antitumor activity.

We evaluated the ability of enzastaurin to suppress tumor cell proliferation in culture. Indeed, enzastaurin suppressed the proliferation of U87MG glioblastoma cells, PC-3 prostate carcinoma cells, and HCT116 colon carcinoma cells in the low micromolar range (Fig. 1). For HCT116 and U87MG cells in particular, there may be a mild stimulatory effect at concentrations below 1 μmol/L, although the relevance of this observation is unclear.

Evaluation of the NCI 60 cell line panel also showed the antiproliferative activity of enzastaurin in the low micromolar range in a wide variety of cancer cell lines: leukemia (K562 and MOLT-4), non–small cell lung cancer (A549, EKVX, and HOP-92), colon cancer (COLO205, HCT116, KM12, and SW-620), central nervous system cancer (SF-295, SF-539, and U251), melanoma (LOXIMVI, M14, SK-MEL-5, SK-MEL-28, and UACC-257), ovarian cancer (OVCAR-3, OVCAR-4, and OVCAR-8), renal cancer (CAKI-1), prostate cancer (PC-3), and breast cancer (MCF-7, NCI/ADR-RES, and MDA-MB-435). The cell lines most sensitive to enzastaurin were K-562, MOLT-4, HOP-92, and PC-3. Cell lines of the NCI 60 cell line panel that were unaffected by enzastaurin include the prostate cancer cell line DU-145; the breast cancer cell lines HS-578T, BT-549, and T-47D; the melanoma cell line MALME-3M; lung cancer cell lines HOP-62, NCI-H23, NCI-H322M, and NCI-460; the ovarian cancer cell lines OVCAR-5 and SK-OV-3; and the renal cancer cell lines 786-0, A498, ACHN, RXF393, and TK-10 (data not shown). These data collectively show that enzastaurin suppresses the proliferation of a wide array of cancer cell lines in the low micromolar range, the same concentration range achieved in the plasma of clinical trials patients (21).

We next sought to determine whether enzastaurin might induce apoptosis in tumor cells. As measured by oligonucleosomal fragmentation, enzastaurin induced apoptosis in both HCT116 colon carcinoma cells and U87MG glioblastoma cells in the low micromolar range (Fig. 2*A*). To confirm these results, we also evaluated apoptosis by TUNEL staining. Enzastaurin treatment of HCT116 colon carcinoma cells induced apoptosis in a dose-dependent manner with the percentage of TUNEL positive cells increasing from a basal level of roughly 2% to >50% in HCT116 cells treated with 4 μmol/L enzastaurin (Fig. 2*B*). Apoptosis was also evident by examining the sub-G_0-G_1 fraction after fluorescence activated cell sorting in HCT116 cells (data not shown). These analyses show that enzastaurin induces apoptosis in cultured human cancer cell lines in the low micromolar range (1-4 μmol/L).

Enzastaurin blocks phosphorylation of GSK3β and ribosomal protein S6. Enzastaurin was developed as an ATP-competitive, PKCβ-selective small-molecule inhibitor with an IC_{50} for PKCβ of 6 nmol/L. Phase I clinical trials showed that the 525 mg/d

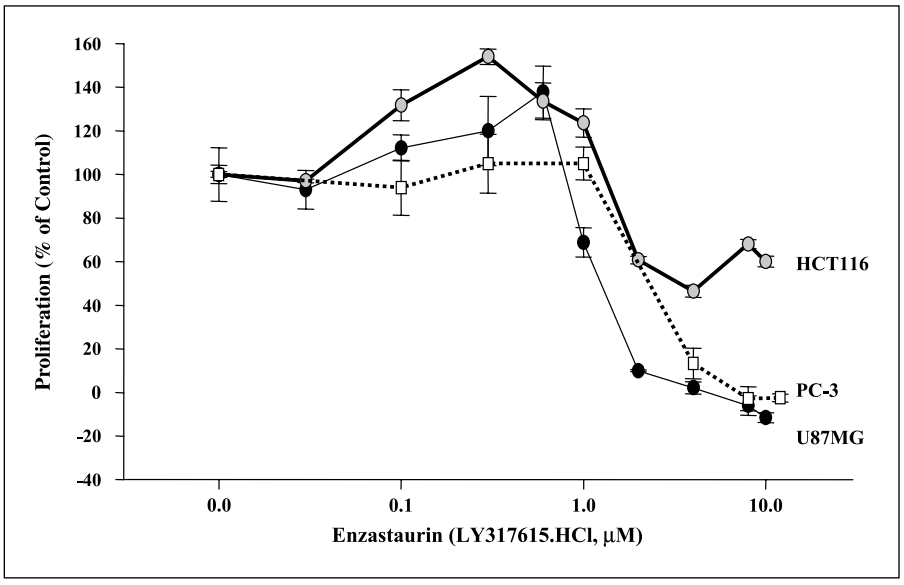

Figure 1. Antiproliferative activity of enzastaurin. PC-3 prostate cancer, HCT116 colon cancer, and U87MG glioblastoma cell lines were incubated with enzastaurin for 6 days in media supplemented with 1% FBS. Proliferation was scored by staining with PI as described in Materials and Methods.

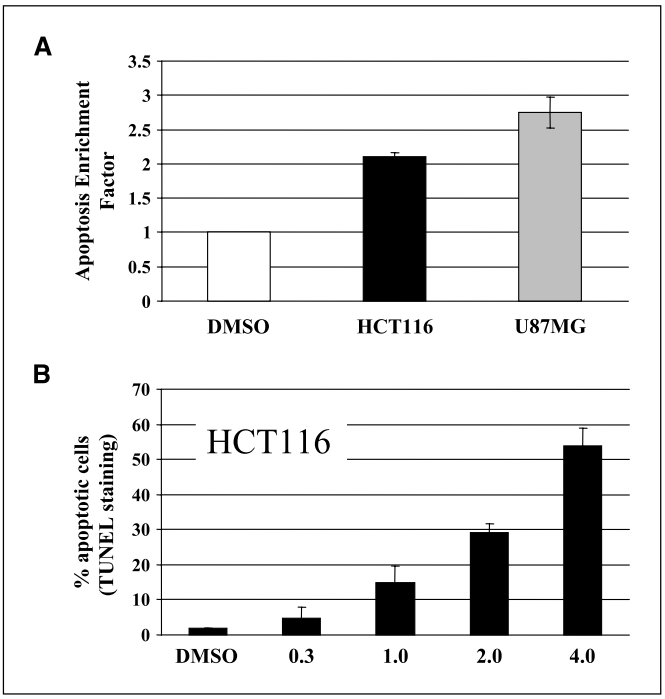

Figure 2. Proapoptotic activity of enzastaurin. *A,* HCT116 colon cancer and U87MG glioblastoma cells were incubated with 4 μmol/L enzastaurin for 48 hours in media supplemented with 1% FBS. Apoptosis was determined using the Cell Death Detection ELISA (Roche Applied Science). *B,* HCT116 colon cancer cells were incubated with enzastaurin (0.3-4 μmol/L) for 72 hours in media supplemented with 1% FBS. Apoptosis was determined by TUNEL staining using the *in situ* cell death detection kit (Roche Applied Science).

dose yields steady-state plasma concentrations of enzastaurin and its analytes up to 8 μmol/L, with the mean plasma exposure of nearly 2 μmol/L (21). To understand better the activity of enzastaurin in this concentration range, we profiled *in vitro* activity against other kinases at 1 μmol/L (Table 2, Upstate kinase profiler). At this concentration, enzastaurin inhibits the activity of PKCβ, PKCγ, PKCδ, PKCθ, PKCξ, and PKCε by ~90% or more but did not show substantial inhibition of PKCμ and PKCι. At 1 μmol/L, enzastaurin also suppressed the activity of p70S6 kinase, PKCζ, and PKCη by nearly 50% but failed to show substantial inhibition of other serine-threonine kinases (IKKα and IKKβ, c-*jun* NH_2-terminal kinases, MKKs, stress-activated protein kinases, mitogen-activated protein kinases, AMPK, PRK2, PKBα, PKBβ, or PDK1) or tyrosine kinases (epidermal growth factor receptor, platelet-derived growth factor receptor, fibroblast growth factor receptor, BTK, SRC, Abl; Table 2). These data reaffirm that enzastaurin selectively inhibits PKCβ at low concentrations and inhibits the activity of other PKC isozymes at higher concentrations, concentrations that are reached or surpassed in clinical trials.

We therefore sought to examine whether pathways known to be influenced by PKC activity might be affected in human tumor cells by enzastaurin treatment. PKC activity has been connected to many intracellular signaling cascades, including the ras-ERK signaling axis (1, 9) and the PI3K/AKT pathway (1, 8, 10–13). Treatment of HCT116 colon carcinoma cells and U87MG glioblastoma cells with 1 μmol/L enzastaurin failed to inhibit ERK activity, as detected by western blotting with phospho-ERK antibodies (data not shown). In contrast, enzastaurin treatment showed a clear, time-dependent reduction of $GSK3\beta^{Ser9}$ phosphorylation in HCT116 cells (Fig. 3*A*). Enzastaurin treatment similarly inhibits $GSK3\beta^{Ser9}$ phosphorylation in other cultured human tumor cells, including U87MG glioblastoma cells, HT-29 colon carcinoma cells, Raji lymphoma cells, and PC-3 prostate carcinoma cells (data not shown).

Phosphorylation of $GSK3\beta^{Ser9}$ has been linked to PKCβ activity (8, 14, 15) and could therefore be blocked by enzastaurin treatment. Phosphorylation of $GSK3\beta^{Ser9}$ has also been repeatedly linked to AKT activity (16). As such, the suppression of $GSK3\beta^{Ser9}$ phosphorylation may reflect inhibition of PKCs as well as the AKT pathway. Indeed, the PKC inhibitor PKC412 also suppresses $GSK3\beta^{Ser9}$ phosphorylation by influencing AKT pathway signaling, although the mechanism for this is not completely understood (22). Consistent with the possibility that enzastaurin affects the AKT signaling pathway, enzastaurin also suppressed the phosphorylation of ribosomal protein $S6^{Ser240/244}$ (Fig. 3*B*) and of AKT^{Thr308} (Fig. 3*C*), although the time course for these events was delayed relative to the inhibition of $GSK3\beta^{Ser9}$ phosphorylation.

Oral dosing of enzastaurin suppresses human tumor xenograft growth and $GSK3\beta^{Ser9}$ phosphorylation. The phase I clinical trials for enzastaurin have shown that oral administration at 525 mg/d yields ~2 μmol/L mean steady-state plasma exposure of enzastaurin and its analytes (21). To examine more fully the effects of orally given enzastaurin on the growth of human tumor xenografts, we sought to identify a dose that would yield levels of enzastaurin and its metabolites comparable with what is reached in clinical trials. We chose a dose of 75 mg/kg given orally by gavage twice daily. Xenograft-bearing mice were treated for 21 consecutive days starting when the mean tumor volume reached ~100 mm^3. Enzastaurin treatment significantly suppressed the growth of both HCT116 colon carcinoma (Fig. 4*A*) and U87MG glioblastoma (Fig. 5*A*) xenografts ($P < 0.01$ for both studies). In the HCT116 xenograft-bearing mice, plasma exposure for enzastaurin was ~2 μmol/L at 30 minutes,

Table 2. Upstate Kinase Profiler data for enzastaurin (LY317615.HCl, 1 μmol/L)

Kinase	% Control activity	Kinase	% Control activity
PKCβII	11	SAPK2b	96
PKCα	23	SAPK2α	101
PKCγ	10	SAPK3	88
PKCδ	8	SAPK4	97
PKCθ	2	JNK1α1	107
PKCζ	47	JNK2α2	103
PKCε	9	JNK3	85
PKCη	53	MAPK1	114
PKCμ	90	MAPK2	104
PKCι	91	AMPK	91
IKKα	107	PRK2	88
IKKβ	116	Abl	96
MEK1	91	FGFR3	82
MKK6	99	PDGFRα	86
MKK7β	102	PDGFRβ	100
PKBα	75	c-SRC	101
PKBβ	100	BTK	95
PDK1	81	IGF1R	94
p70S6K	52	EGFR	102

Abbreviations: SAPK, stress-activated protein kinase; JNK, c-*jun* NH_2-terminal kinase; MAPK, mitogen-activated protein kinase; MEK, MAPK kinase; EGFR, epidermal growth factor receptor; PDGFR, platelet-derived growth factor receptor; FGFR, fibroblast growth factor receptor.

increased to nearly 3 μmol/L at 1 hour, and dropped to 1.5 μmol/L by 2 hours. Between 8 and 12 hours after dosing, the plasma concentrations of enzastaurin were nearly undetectable (Fig. 4*B*). The time course for enzastaurin plasma exposure was similar on day 1 and on day 21 after dosing (Fig. 4*B*). The time course for plasma exposure of enzastaurin dosed orally in mouse models consistently reflects the data in Fig. 4*B*, with nearly undetectable levels of drug in plasma between 8 and 12 hours after dosing. Consequently, 12-hour time points were not included in further studies.

Enzastaurin robustly suppressed GSK3β^{Ser9} phosphorylation in cultured tumor cells (Fig. 3). We therefore sought to determine whether GSK3β^{Ser9} phosphorylation would be similarly suppressed in xenograft tumor tissues after enzastaurin dosing. Western blot analysis of HCT116 colon cancer xenograft tissues showed that GSK3β^{Ser9} phosphorylation was suppressed in a time-dependent manner after enzastaurin treatment (Fig. 4*C*). The time course for reduction in GSK3β^{Ser9} phosphorylation lags slightly behind the time course for plasma exposure as expected. GSK3β^{Ser9} phosphorylation returned to pretreatment levels at 12 hours after dosing, when plasma exposure levels of enzastaurin were nearly undetectable.

In both cultured tumor cells and in xenograft tumor tissues from the same cell lines, enzastaurin treatment suppressed GSK3β^{Ser9} phosphorylation, indicating that GSK3β^{Ser9} phosphorylation may serve as a reliable marker for enzastaurin activity. To do higher throughput analyses for GSK3β^{Ser9} phosphorylation, we chose a commercially available ELISA detection method (Assay Designs). ELISA analyses of U87MG xenograft tissues revealed >50% reduction in GSK3β^{Ser9} phosphorylation evident at the 2-hour time point and persisting through 8 hours (Fig. 5*B*; $P < 0.0001$ for all time points). In HCT116 xenograft tissues, ELISA analyses showed that GSK3β^{Ser9} phosphorylation was reduced by 50% after 30 minutes and by 80% at 2 hours. Consistent with the western blotting data (Fig. 4*C*), the reduction in GSK3β^{Ser9} phosphorylation persisted through 8 hours. Results for GSK3β^{Ser9} phosphorylation were comparable by western blotting and by ELISA (Fig. 4*C* versus Fig. 6), although the extent of reduction may be more pronounced by western blotting (compare 8-hour time points in Fig. 4*C* and Fig. 6). The differences in the extent to which GSK3β^{Ser9} phosphorylation was reduced in U87MG glioblastoma and HCT116 colon carcinoma xenografts may reflect an inherent difference in the biology of these tumors (for instance, U87MG lacks PTEN expression). Alternately, these data may simply reflect differences in these xenografted tumors related to tumor content, host tissue content, etc. In any case, both xenograft models show a significant, reproducible reduction in GSK3β^{Ser9} phosphorylation evident no later than 2 hours and persisting through 8 hours after oral dosing with enzastaurin.

Enzastaurin suppresses GSK3β^{Ser9} phosphorylation in both xenograft tissues and peripheral blood mononuclear cells. We next sought to determine whether enzastaurin could affect GSK3β^{Ser9} phosphorylation in PBMCs and whether this effect may

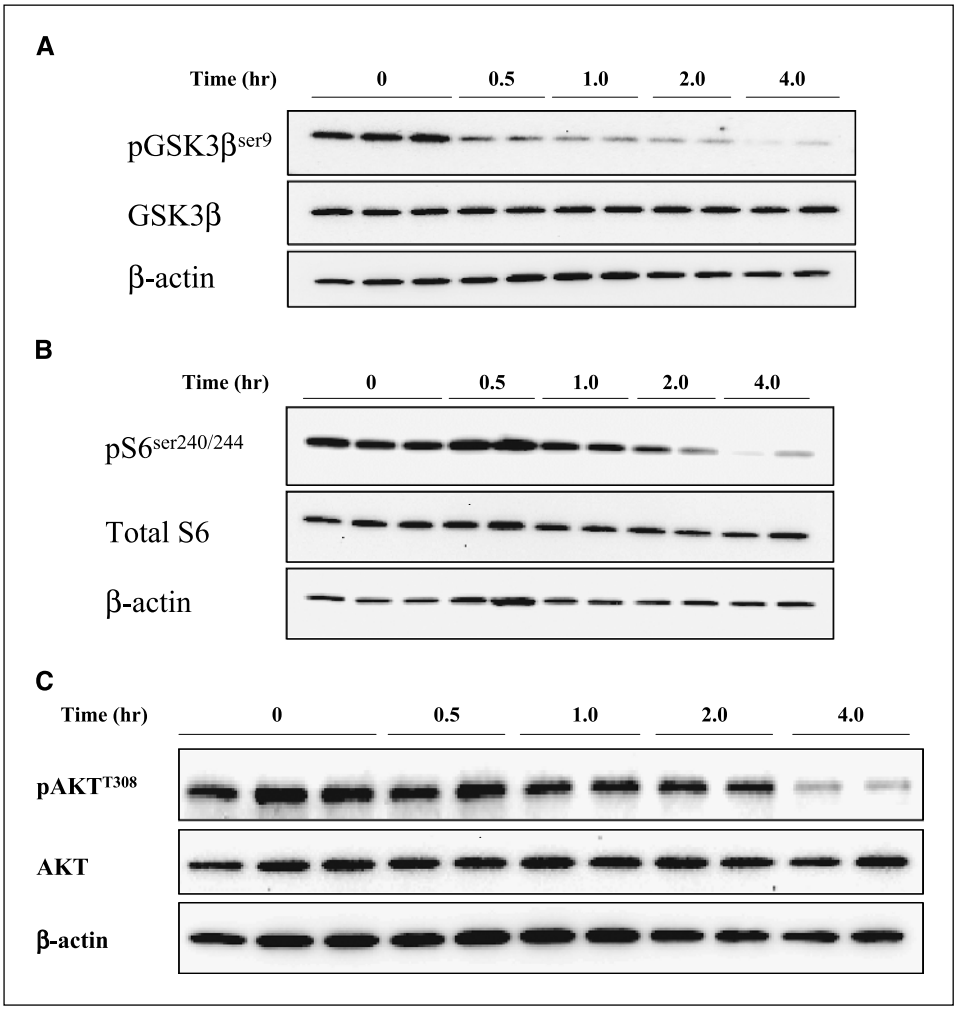

Figure 3. Enzastaurin suppresses cell signaling within the AKT pathway. HCT116 colon cancer cells were incubated with 1 μmol/L enzastaurin in media supplemented with 1% FBS up to 4 hours as indicated. Western blot analyses were performed for the phosphorylation of (*A*) GSK3β at Ser^{9}, (*B*) ribosomal protein S6 at Ser$^{240/244}$, and (*C*) AKT at Thr^{308} (Cell Signaling Technologies). Duplicate blots were run simultaneously and probed for (*A*) GSK3β total protein (BD Transduction), (*B*) ribosomal S6 protein (Cell Signaling Technologies), and (*C*) total AKT protein (BD Transduction). All blots were reprobed for β-actin expression to control for protein loading and transfer differences.

reflect the time course and degree of reduction evident in xenograft tumor tissue. ELISA analyses revealed that GSK3β^{Ser9} phosphorylation is significantly reduced in the PBMCs of xenograft-bearing mice, with the most profound reduction (>60%) between 2 and 4 hours after dosing ($P < 0.005$ up to 4 hours after dose). Similarly, GSK3β^{Ser9} phosphorylation was also significantly reduced in the xenograft tissues harvested from these same mice, again with the most profound reduction (>60%) between 2 and 4 hours after dosing ($P < 0.0001$ up to 4 hours after dosing). These data indicate that the reduction in GSK3β^{Ser9} phosphorylation from the PBMCs of treated mice reflects the time course and extent to which GSK3β^{Ser9} phosphorylation is reduced in xenograft tumor tissues.

Discussion

PKC activity has been implicated in the regulation of tumor-induced angiogenesis, tumor cell proliferation, apoptosis, and tumor

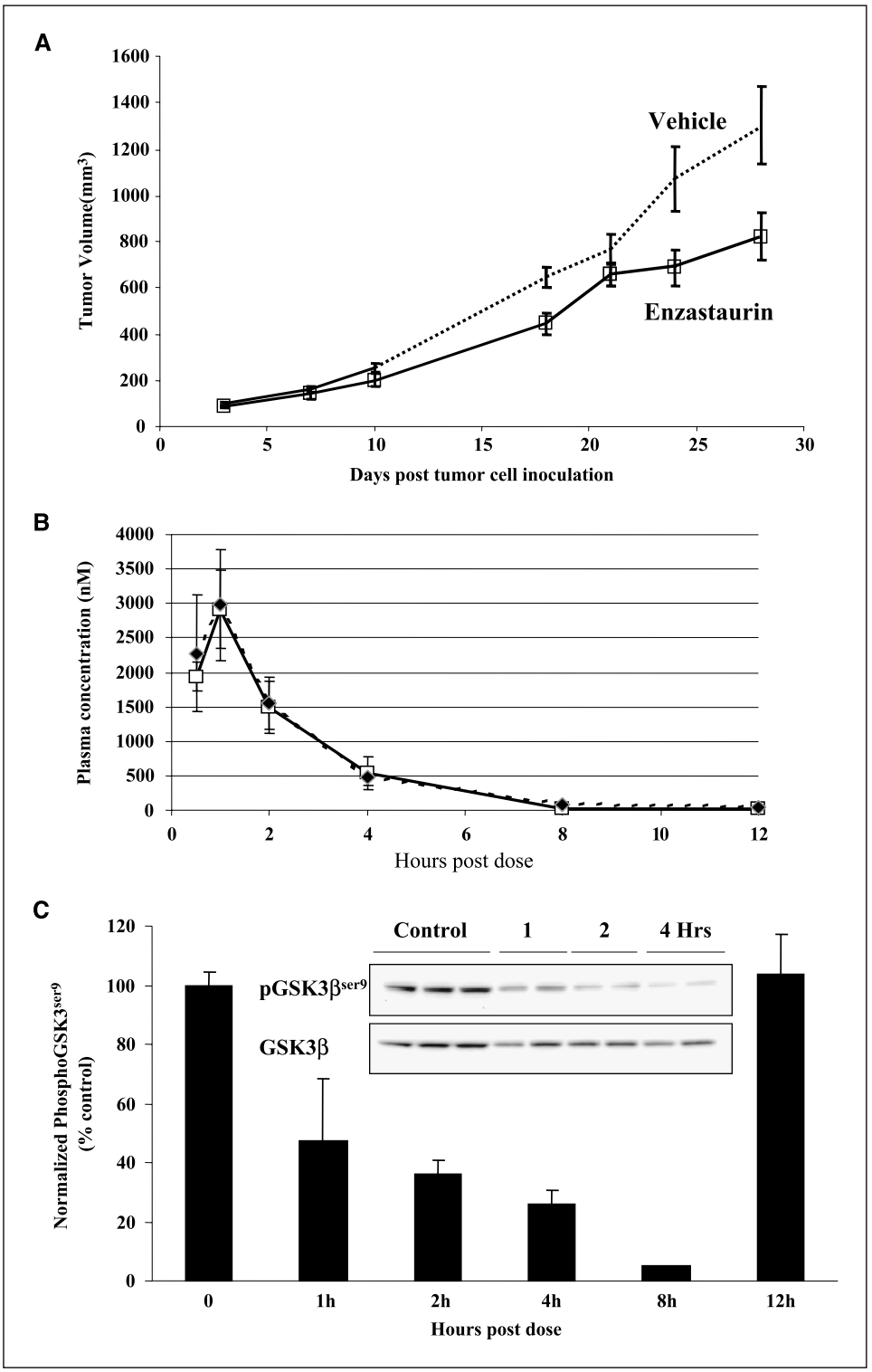

Figure 4. Oral dosing with enzastaurin suppresses xenograft tumor growth and GSK3β phosphorylation. Athymic nude mice bearing HCT116 colon cancer xenografts were treated with 75 mg/kg enzastaurin twice daily by gavage after tumors reached a mean tumor volume of 100 mm^3 ($n = 9$ for each group). *A,* tumor diameter was measured by caliper and tumor volume was calculated according to the formula $A^2 \times B \times 0.536$, where *A* equals the smallest diameter and *B* equals the largest diameter. Tumor growth was significantly suppressed by enzastaurin treatment ($P < 0.01$, two-way repeated measures of variance). *B,* plasma was harvested from tumor bearing mice on day 1 (□) and day 21 (♦) of dosing at 0.5, 1, 2, 4, 8, and 12 hours after dose. Plasma concentrations for enzastaurin were assessed by liquid chromatography tandem mass spectrometry. *C,* on day 21 of dosing, mice were killed and tumors harvested at 0.5, 1, 2, 4, 8, and 12 hours after dose. GSK3β^{Ser9} phosphorylation was assessed from these protein lysates by western blotting.

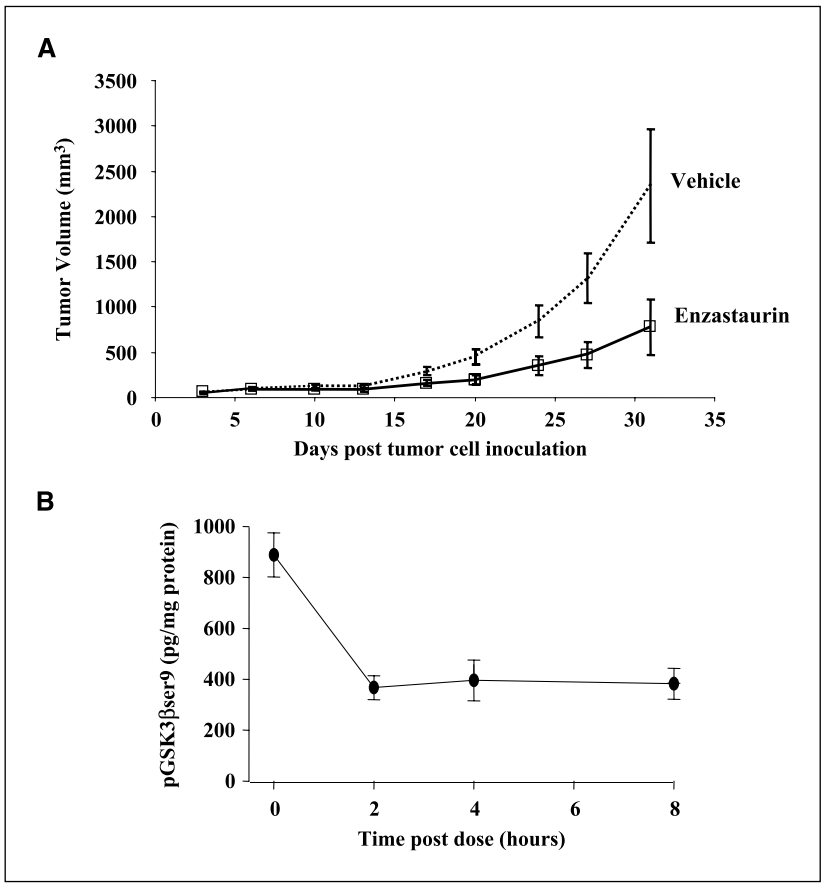

Figure 5. Oral dosing with enzastaurin suppresses xenograft tumor growth and GSK3β phosphorylation. Athymic nude mice bearing U87MG glioblastomas xenografts were treated with 75 mg/kg enzastaurin twice daily by gavage after tumors reached a mean tumor volume of 100 mm^3 (n = 9 for each group). *A,* tumor diameter was measured by caliper and tumor volume was calculated according to the formula $A^2 \times B \times 0.536$, where A equals the smallest diameter and B equals the largest diameter. Tumor growth was significantly suppressed by enzastaurin treatment ($P < 0.01$, two-way repeated measures of variance). *B,* on day 21 of dosing, tumors were harvested at 2, 4, or 8 hours after dose and protein lysates were subjected to ELISA analysis for $GSK3\beta^{Ser9}$ phosphorylation. $GSK3\beta^{Ser9}$ phosphorylation was significantly reduced versus Vehicle control tumors at all time points ($P < 0.001$, Dunnett's method, ANOVA).

invasiveness (1). On this basis, a number of PKC inhibitors have been advanced into clinical trials for the treatment of human cancers. Enzastaurin was developed as an ATP-competitive, selective inhibitor of PKCβ. Early studies showed that enzastaurin profoundly suppressed VEGF-induced angiogenesis. Enzastaurin dramatically suppressed the growth of new vasculature towards a VEGF-impregnated disc implanted in the rat corneal micropocket (18). These findings are consistent with the role for PKCβ in mediating the VEGF-induced proliferative signals in endothelial cells (1, 3). Based in part on this robust antiangiogenic activity, enzastaurin was advanced into clinical trials as a novel anticancer therapy.

We now show that enzastaurin also exhibits a direct effect on human tumor cells, inducing apoptosis in, and suppressing proliferation of, a wide array of cultured human tumor cells. Enzastaurin treatment interferes with signaling through the AKT pathway, suppressing the phosphorylation of $GSK3\beta^{Ser9}$, ribosomal protein $S6^{Ser240/244}$, and AKT^{Thr308}. The suppression of $GSK3\beta^{Ser9}$ phosphorylation by enzastaurin was also evident in human xenograft tissues. Oral dosing of xenograft-bearing mice with enzastaurin (to achieve plasma exposure levels similar to that reached in human clinical trials) suppressed $GSK3\beta^{Ser9}$ phosphorylation by >50% in both colon cancer and glioblastoma xenografts. $GSK3\beta^{Ser9}$ phosphorylation was reduced in these tissues in a time-dependent manner, coinciding with plasma exposure levels of enzastaurin. Phosphorylation of $GSK3\beta^{Ser9}$ was suppressed in the PBMCs of these xenograft-bearing mice to a similar extent and with a similar time course as in the xenograft tumor tissue, suggesting that $GSK3\beta^{Ser9}$ phosphorylation in PBMCs may serve as a reliable pharmacodynamic marker for enzastaurin activity.

The direct, proapoptotic effects of enzastaurin treatment on human tumor cells were achieved at drug concentrations similar to those achieved in the plasma of clinical trials patients (1-4 μmol/L). At these drug concentrations, enzastaurin treatment interferes with signaling through the PI3K/AKT pathway, suppressing phosphorylation of $GSK3\beta^{Ser9}$, ribosomal protein $S6^{Serine\ 240/244}$, and AKT^{Thr308}.

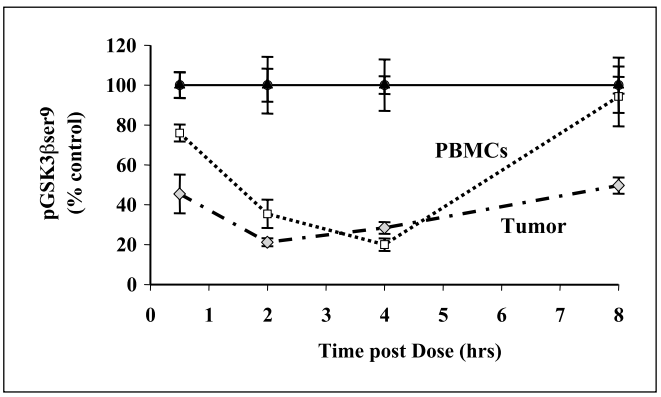

Figure 6. Enzastaurin treatment suppresses GSK3β phosphorylation in PBMCs and tumors. HCT116 tumor tissue and plasma from these xenograft-bearing mice were harvested at 0.5, 2, 4, and 8 hours after dosing with enzastaurin at 75 mg/kg (n = 5 for each time point). Protein lysates from these tissues were subjected to ELISA analyses for GSK3β phosphorylation. GSK3β phosphorylation was significantly reduced in PBMCs at 0.5, 2, and 4 hours ($P < 0.005$, Dunnett's methods, ANOVA) but not 8 hours. GSK3β phosphorylation was significantly reduced in tumor at all time points ($P < 0.0001$ at 0.5-4 hours; $P = 0.018$ at 8 hours, Dunnett's method, ANOVA). Percentage of control for each tissue respectively, with the vehicle-treated tumor or PBMCs set at 100%.

The PI3K/AKT pathway is a key regulator of cellular survival and is frequently activated in many human cancers, most notably glioblastomas, melanomas, and prostate, ovarian, and endometrial carcinomas (23). Interestingly, previous work had indicated that enzastaurin treatment suppressed VEGF expression by tumor xenografts (19). VEGF expression is regulated at both the transcriptional and posttranscriptional levels through activation of the AKT pathway (24–26).

It is unclear how enzastaurin may interfere with signaling through the PI3K/AKT pathway. In *in vitro* kinase assays, enzastaurin shows minimal inhibitory activity against p70S6 kinase and virtually no inhibition of AKT-1 or PDK-1, suggesting that the kinases responsible for phosphorylation of GSK3β^{Ser9}, ribosomal protein S6$^{Ser240/244}$, and AKT^{Thr308} may not be directly inhibited by enzastaurin (LY317615.HCl). Furthermore, the time course for these signaling changes is different. Decreased phosphorylation of GSK3β^{Ser9} is evident within 30 minutes, whereas decreased phosphorylation of ribosomal protein S6$^{Ser240/244}$ and AKT^{Thr308} is evident at 2 and 4 hours post-treatment, respectively. Collectively, these data suggest that enzastaurin may indirectly suppress signaling through the AKT pathway. The PKC inhibitor PKC412 has also been shown to suppress AKT pathway signaling, upstream or at the level of AKT, although no direct mechanism was clear in these studies either (22).

Recent evidence has now shown that various PKC family members can regulate AKT activity. PKCα can regulate the activity of AKT by directly stimulating phosphorylation of Ser^{473} in endothelial cells (11). PKCβII can also directly phosphorylate and activate AKT in mast cells (12). Activation of PKCη can also activate AKT in glioblastoma cells, supporting glioblastoma proliferation (13). Our data show that the AKT pathway is suppressed in cells treated with 1 to 4 μmol/L enzastaurin. At these concentrations, enzastaurin can directly suppress the kinase activity of multiple PKC isoforms. It is therefore conceivable that interference with the AKT signaling pathway may be related to the effect of enzastaurin on multiple PKC family members.

Enzastaurin has now successfully advanced to phase II clinical trials for the treatment of refractory glioblastoma and DLBCL. With this report, we now show that enzastaurin exhibits direct antitumor activity, inducing tumor cell apoptosis and suppressing tumor cell proliferation. Moreover, enzastaurin interferes with signaling through the AKT pathway, a pathway frequently activated in a variety of human cancers. Finally, we show that enzastaurin profoundly suppresses the phosphorylation of GSK3β^{Ser9} both in human tumor xenograft tissue and in PBMCs harvested from xenograft-bearing mice, suggesting that GSK3β^{Ser9} phosphorylation may serve as a reliable pharmacodynamic marker of enzastaurin activity. With previous data, these data show that enzastaurin suppresses tumor growth through multiple mechanisms- the direct induction of tumor cell death and the suppression of tumor cell proliferation coupled to the indirect effect of suppressing tumor-induced angiogenesis.

Acknowledgments

Received 1/11/2005; revised 3/31/2005; accepted 5/27/2005.

The costs of publication of this article were defrayed in part by the payment of page charges. This article must therefore be hereby marked *advertisement* in accordance with 18 U.S.C. Section 1734 solely to indicate this fact.

We thank Drs. Richard Gaynor, Kerry Blanchard, Jake Starling, John McDonald, Homer Pearce, Christopher Slapak, and Alan Hatfield for supporting this work and Cecile Gonzalez-Cerimele for all of her assistance.

References

1. Goekjian PG, Jirousek MR. Protein kinase C inhibitors as novel anticancer drugs. Expert Opin Investig Drugs 2001;10:2117–40.
2. Castagna M, Takai Y, Kaibuchi K, Sano K, Kikkawa U, Nishizuka Y. Direct activation of calcium-activated, phospholipid-dependent protein kinase by tumor-promoting phorbol esters. J Biol Chem 1982;257:7847–51.
3. Yoshiji H, Kuriyama S, Ways DK, et al. Protein kinase C lies on the signaling pathway for vascular endothelial growth factor-mediated tumor development and angiogenesis. Cancer Res 1999;59:4413–8.
4. Shipp MA, Ross KN, Tamayo P, et al. Diffuse large B-cell lymphoma outcome prediction by gene-expression profiling and supervised machine learning. Nat Med 2002;8:68–74.
5. da Rocha AB, Mans DR, Regner A, Schwartsmann G. Targeting protein kinase C: new therapeutic opportunities against high-grade malignant gliomas? Oncologist 2002;7:17–33.
6. Gokmen-Polar Y, Murray NR, Velasco MA, Gatalica Z, Fields AP. Elevated protein kinase C βII is an early promotive event in colon carcinogenesis. Cancer Res 2001;61:1375–81.
7. Su TT, Guo B, Kawakami Y, et al. PKC-β controls I κ B kinase lipid raft recruitment and activation in response to BCR signaling. Nat Immunol 2002;3:780–6.
8. Murray NR, Davidson LA, Chapkin RS, Clay Gustafson W, Schattenberg DG, Fields AP. Overexpression of protein kinase C βII induces colonic hyperproliferation and increased sensitivity to colon carcinogenesis. J Cell Biol 1999;145:699–711.
9. Zhang J, Anastasiadis PZ, Liu Y, Thompson EA, Fields AP. Protein kinase C (PKC) βII induces cell invasion through a Ras/Mek-, PKC iota/Rac 1-dependent signaling pathway. J Biol Chem 2004;279:22118–23. Epub 2004 Mar 22.
10. Balendran A, Hare GR, Kieloch A, Williams MR, Alessi DR. Further evidence that 3-phosphoinositide-dependent protein kinase-1 (PDK1) is required for the stability and phosphorylation of protein kinase C (PKC) isoforms. FEBS Lett 2000;484:217–23.
11. Partovian C, Simons M. Regulation of protein kinase B/Akt activity and Ser^{473} phosphorylation by protein kinase Cα in endothelial cells. Cell Signal 2004; 16:951–7.
12. Kawakami Y, Nishimoto H, Kitaura J, et al. Protein kinase C βII regulates Akt phosphorylation on Ser-473 in a cell type- and stimulus-specific fashion. J Biol Chem 2004;279:47720–5. Epub 2004 Sep 09.
13. Aeder SE, Martin PM, Soh JW, Hussaini IM. PKC-eta mediates glioblastoma cell proliferation through the Akt and mTOR signaling pathways. Oncogene 2004;23: 9062–9.
14. Fang X, Yu S, Tanyi JL, Lu Y, Woodgett JR, Mills GB. Convergence of multiple signaling cascades at glycogen synthase kinase 3: Edg receptor-mediated phosphorylation and inactivation by lysophosphatidic acid through a protein kinase C-dependent intracellular pathway. Mol Cell Biol 2002;22:2099–110.
15. Goode N, Hughes K, Woodgett JR, Parker PJ. Differential regulation of glycogen synthase kinase-3 β by protein kinase C isotypes. J Biol Chem 1992;267:16878–82.
16. Cross DA, Alessi DR, Cohen P, Andjelkovich M, Hemmings BA. Inhibition of glycogen synthase kinase-3 by insulin mediated by protein kinase B. Nature 1995; 378:785–9.
17. Faul MM, Gillig JR, Jirousek MR, et al. Acyclic *N*-(azacycloalkyl)bisindolylmaleimides: isozyme selective inhibitors of PKCβ. Bioorg Med Chem Lett 2003;13: 1857–9.
18. Teicher BA, Alvarez E, Menon K, et al. Antiangiogenic effects of a protein kinase C β-selective small molecule. Cancer Chemother Pharmacol 2002;49:69–77.
19. Keyes KA, Mann L, Sherman M, et al. LY317615 decreases plasma VEGF levels in human tumor xenograft-bearing mice. Cancer Chemother Pharmacol 2004;53:133–40. Epub 2003 Oct 31.
20. Graff JR, Konicek BW, McNulty AM, et al. Increased AKT activity contributes to prostate cancer progression by dramatically accelerating prostate tumor growth and diminishing p27Kip1 expression. J Biol Chem 2000;275: 24500–5.
21. Herbst RS, Thornton DE, Kies MS, et al. Phase 1 study of LY317615, a protein kinase Cβ inhibitor. Proc of ASCO 2002;21:82a.
22. Tenzer A, Zingg D, Rocha S, et al. The phosphatidylinositide 3′-kinase/Akt survival pathway is a target for the anticancer and radiosensitizing agent PKC412, an inhibitor of protein kinase C. Cancer Res 2001;61: 8203–10.
23. Sansal I, Sellers WR. The biology and clinical relevance of the PTEN tumor suppressor pathway. J Clin Oncol 2004;22:2954–63.
24. De Benedetti A, Harris AL. eIF4E expression in tumors: its possible role in progression of malignancies. Int J Biochem Cell Biol 1999;31:59–72.
25. Pore N, Liu S, Shu HK, et al. Sp1 is involved in Akt-mediated induction of VEGF expression through an HIF-1-independent mechanism. Mol Biol Cell 2004;15: 4841–53. Epub 2004 Sep 01.
26. Skinner HD, Zheng JZ, Fang J, Agani F, Jiang BH. Vascular endothelial growth factor transcriptional activation is mediated by hypoxia-inducible factor 1α, HDM2, and p70S6K1 in response to phosphatidylinositol 3-kinase/AKT signaling. J Biol Chem 2004;279:45643–51. Epub 2004 Aug 26.

The Protein Kinase Cβ–Selective Inhibitor, Enzastaurin (LY317615.HCl), Suppresses Signaling through the AKT Pathway, Induces Apoptosis, and Suppresses Growth of Human Colon Cancer and Glioblastoma Xenografts

Jeremy R. Graff, Ann M. McNulty, Kimberly Ross Hanna, et al.

Cancer Res 2005;65:7462-7469.